The Molecular Structure of Low-Density Polyethylene. 2. Particle Scattering Factors

E. Nordmeier,* U. Lanver, and M. D. Lechner

Department of Physical Chemistry, University of Osnabrück, 4500 Osnabrück, FRG.
Received August 19, 1988; Revised Manuscript Received April 13, 1989

ABSTRACT: In order to characterize branched low-density polyethylenes (LDPE 1, LDPE 3, and Lupolen 1840 D) by means of light scattering, particle scattering factors for different branched structures were calculated and compared with experimentally determined values. Three models were considered in some detail: (i) heterogeneous combs with branches of equal length; (ii) combs, monodisperse with respect to the molar mass and polydisperse with respect to the length of a branch; (iii) random branched polymer trees of the kind A_2–B_x. Additionally, the results were analyzed by means of space correlation functions. For LDPE 1 and LDPE 3 it was found that the comb models describe the observed particle scattering factors quite well. Best-fit values of the number of long branches per molecule, n_b, agree well with those derived from the g ratio, which is defined as the ratio of the square radii of gyration of a branched to a linear macromolecule, both containing equal number of segments. The molecular structure of Lupolen 1840 D in some respects is that of a comb and in others is that of a polymer tree, of the kind A_2–B_x. Superimposement of particle scattering factors, assigned to these structures, gives the best measure of agreement between theory and experiment.

Introduction

Light will be scattered by a molecule in solution if the molecule has a polarizability different from its surroundings. In this case, the oscillating dipole moment, induced by the electric field of the incident light beam, will radiate light in all directions. Destructive interference occurs. As a result, the intensity of the scattered light will vary depending on the size of the scattering molecule and the magnitude of the scattering vector, $q = (4\pi/\lambda') \sin(\theta/2)$. Here, λ' is the wavelength in the medium, and θ is the scattering angle. The ratio of the scattered light intensity I_θ at the scattering angle θ to the extrapolated zero angle scattered light intensity I_0 is called the particle scattering factor $P(q)$.

$P(q)$ can be presented by eq 1, where N is the total

$$P(q) = 1/N^2 \sum_{i=1}^{N} \sum_{j=1}^{N} \left\langle \frac{\sin(qr_{ij})}{qr_{ij}} \right\rangle \tag{1}$$

number of segments per chain and r_{ij} is the distance between segments i and j. The angular brackets are related to the changes in the configurations of the chain brought on by the flexibility of its segments. If the Gaussian distribution function is used for r_{ij}

$$w(r_{ij}) = ({}^3/_2\pi\langle r_{ij}^2\rangle)^{3/2} \exp(-3r_{ij}^2/2\langle r_{ij}^2\rangle) 4\pi r_{ij}^2 \tag{2}$$

eq 1 yields the result

$$\langle(\sin(qr_{ij}))/(qr_{ij})\rangle = \exp(q^2\overline{r_{ij}^2}/6)$$

Thus it holds that

$$P(q) = (1/N^2) \sum_{i=1}^{N} \sum_{j=1}^{N} \exp(q^2\overline{r_{ij}^2}/6) \tag{3}$$

The exact form of the particle scattering factor depends on the special molecular structure of the macromolecule. For instance, Debye[1] made the assumption, consistent with linear macromolecules and Gaussian statistics, that $\langle r_{ij}^2\rangle = |i-j|b^2$, where b is the length of a segment. He thus obtained the famous result

$$P(q) = (2/x^2)(\exp(-x) - 1 + x) \tag{4}$$

where $x = 16\pi^2\langle S^2\rangle(\sin(\theta/2)/\lambda')^2$. Here, $\langle S^2\rangle$ is the mean-square radius of gyration. Equation 4 is called the Debye function.

In any other case, especially in the case of branched molecular structures, the evaluation of $P(q)$ is much more complicated than stated by Debye. A problem is how the double sum in eq 3 can be evaluated, since the difficulties are mainly of a combinative nature. Therefore different calculation techniques have been developed, where Debye's technique, the theory of the cascade process,[2] and the percolation theory[3] are essential. The great advantage of the cascade theory compared with Debye's technique is that it reduces the use of probability theory by introducing the concept of a statistical forest of polymer trees, defined by the probability generating function for the number of offsprings in each generation. Also with respect to this theory the understanding of the combined effects of branching and polydispersity on various physical properties is advanced. On the other hand, percolation simulations on a computer demonstrate nicely the formation of a well-defined surface,[4] whereas the prediction of the gel point still remains poor.

It is the purpose of this paper to compare experimental values of $P(q)$ estimated for branched low-density polyethylenes, studied in the preceding paper,[5] which those computed here for model structures. Thereby we can draw conclusions concerning the branching structure of low-density polyethylene.

Obviously, quite a large number of different branched structures are conceivable, even if the fraction of the branching units in the polymer is kept constant. A selection is indispensable. According to ref 5 there are three groups of branched structures which are of special interest: (i) heterogeneous combs, with branches of equal length; (ii) combs, monodisperse with respect to the molar mass and polydisperse with respect to the length of a branch; (iii) random branched polymer trees of the kind A_2–B_x. In order to derive theoretical expressions for $P(q)$ concerning these models, we make use of Debye's technique and the theory of the cascade process. Percolation the-

* To whom correspondence should be addressed.

0024-9297/90/2223-1077$02.50/0

ory yields results, which are in some detail ambiguous. In addition, we evaluate the Fourier transform of the particle scattering factor, which is called the space correlation function and is closely related to the segment-density distribution.

Data Handling

Measurements were made by using vertically polarized light of wavelengths 366, 436, and 546 nm supplied from a medium-pressure mercury lamp. The particle scattering factors at different concentrations were extrapolated to infinite dilution and then superimposed at the three different wavelengths by plotting the normalized curve of $P^{-1}(q)$ against the variable q^2, where q has been corrected for the refractive index of n-decane for T = 130 °C at different wavelengths. It is to be particularly noted that the data points obtained at the three wavelengths overlap smoothly, thus imparting confidence to the important region of the high abscissa values. It should also be noted that the range of abscissa values accessible to measurement by an angular scan has been doubled by extending the wavelength of the incident radiation from 546 nm down to 366 nm. Finally, the mean-square radius of gyration was determined from the slope at infinite dilution of the smooth curve $P^{-1}(q)$ versus q^2. For detailed information we refer to ref 5.

Heterogeneous Combs

The most complete theoretical work on the particle scattering factors of comb macromolecules appeared in 1966, suggested by Casassa and Berry.[6] In the case of heterogeneous combs, formed by the random incorporation of an average number, $\bar{f}$, of monodisperse branches onto a monodisperse backbone, the particle scattering factor is given by

$$P(\Theta)_{\text{hetero}} = \frac{\frac{2}{\bar{u}^2}}{1 + \frac{(1-\bar{\lambda})^2}{\bar{f}}}\left[\bar{u} - (1 - e^{-\bar{u}\bar{\lambda}}) + (1 - e^{-\bar{u}(1-\bar{\lambda})/\bar{f}}) \times \left(\bar{f} - \frac{2(1 - e^{-\bar{u}\bar{\lambda}})}{\bar{u}\bar{\lambda}/\bar{f}}\right) + (1 - e^{-\bar{u}(1-\bar{\lambda})/\bar{f}})^2\left(\frac{\bar{u}\bar{\lambda} - (1 - e^{-\bar{u}\bar{\lambda}})}{(\bar{u}\bar{\lambda}/\bar{f})^2}\right)\right] \quad (5)$$

$\bar{f}$, $\bar{u}$, and $\bar{\lambda}$ are all average values concerning the fact that Casassa and Berry have used a binomial distribution for the number of branches placed on the backbone. This causes a distribution around an average molar mass, which is symptomatic for heterogeneous combs. $\bar{u}$ is defined as $\bar{u} = q^2Nb^2/6$, where N is the total number of segments and b is the length of a segment. Here, X-ray analysis[7] states that b is equal to 10 Å. $\bar{\lambda}$ denotes the ratio N_0/N, where N_0 is the average number of segments building the backbone. In order to compare the experimental values of $P(q)$ with those computed by eq 5, we have to take in account certain important facts, which are stated below.

(1) ^{13}C NMR measurements[5] state that the LDPE's studied here contain both different short branches as well some long branches, where the average number, n_b, of segments per long branch is unknown. Therefore we consider a model polymer composed of several groups of heterogeneous comb molecules, where each group is characterized by combs with branches of equal length. It follows that each group must be associated with its own particle scattering factor. In order to get the particle scattering factor, which describes the whole sample, we have to sum the individual particle scattering factors, after having weighted them to their relative frequency. We can therefore write

$$P(q) = \sum_{i=1}^{n_b} w_i P_i(q)$$

where w_i is the weight factor according to the particle scattering factor $P_i(q)$, which describes a heterogeneous comb, where each branch obtains i segments.

Here, the average number of branches per molecule and the number of segments associated with each branch, except that of a long branch, are known from ^{13}C NMR measurements. Thus, it is necessary to set w_i equal to the relative branching frequency per molecule according to the case that a branch contains i segments. Values of w_i, estimated by this procedure, are listed in Table I.

Finally the unknown parameter n_b may be used as fit parameter, whereby the best-fit values of n_b are summarized in Table II. A discussion of Table II will be included in a later section.

(2) Secondly, we have to take into account the effect of polydispersity. It holds that

$$P(q)_z = \sum_{i=1}^{n_b} w_i\left(\int NP_i(N,q)\, f(N)\, dN\right)/\left(\int Nf(N)\, dN\right) \quad (6)$$

where $f(N)$ denotes the distribution of different degrees of polymerization. In accordance with ref 5, we use the three-parameter distribution, suggested by Hosemann and Schramek. Thereby, it must be noted that the integration of eq 6 cannot be performed explicitly. A useful quadrature is that of Gauss–Laguerre.

(3) Finally, we have to pay attention to the effect of excluded volume, which destroys the Markovian nature of a random coil. Particularly, $\langle r_{ij}^2\rangle$ increases more rapidly with the number of segments, $|i - j|$, as eq 2 states. Therefore, Ptitsyn and Benoit[8] proposed to use a relationship like

$$\langle r_{ij}^2\rangle = |i - j|^{1+\epsilon}b^2 \quad (7)$$

where ϵ is a parameter which is zero in a Θ solvent and greater than zero in a good solvent. Of course, if $\epsilon = 0$ eq 7 reduces to the Debye equation. In order to get ϵ, Ptitsyn and Benoit used the Mark–Houwink equation $[\eta] = KM^a$, where ϵ is equal to $(2a - 1)/3$. $[\eta]$ is called the intrinsic viscosity, and K is a constant, which depends on the short-range interactions inside the chain.

However, several authors[9] found that use of eq 7 seriously overestimates the value of ϵ with regard to fit experimental data of $P(q)$. Therefore, in the case of branched

Table I
Weight Factors w_i

	no. of segments per branch					
sample	1	2	3	4	5	n_b
LDPE 1	0.043	0.295	0.000	0.436	0.113	0.113
LDPE 3	0.088	0.190	0.000	0.454	0.134	0.134
Lupolen 1840 D	0.084	0.305	0.000	0.385	0.120	0.120

Table II
Best-Fit Values of n_b[a]

	sample		
method	LDPE 1	LDPE 3	Lupolen 1840 D
g ratio[5]	32	62	9
psf (eq 6)	28	66	
psf (eq 10)	35	60	

[a] psf = particle scattering factor.

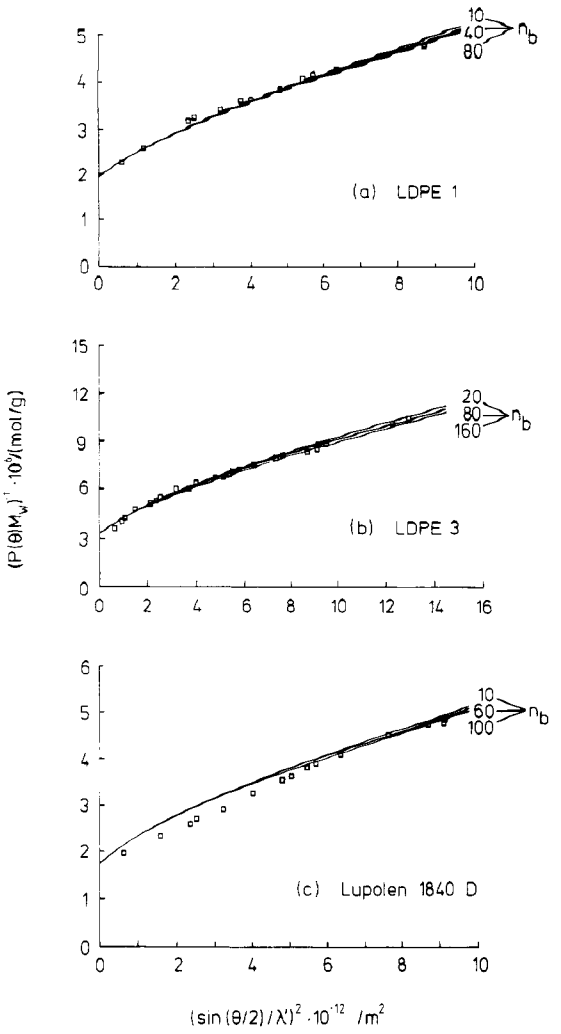

Figure 1. Particle scattering factors calculated by the heterogeneous comb model: (a) LDPE 1, (b) LDPE 3, and (c) Lupolen 1840 D.

molecules, we think it may be better to use a relationship of the form

$$\langle r_{ij}^2 \rangle = \alpha^2 |i-j| b^2 \tag{8}$$

Here, α is the expansion factor, defined as $\alpha = \{\langle S^2 \rangle_z / \langle S^2 \rangle_{z,\Theta}\}^{0.5}$ where $\langle S^2 \rangle_{z,\Theta}$ denotes the mean-square radius of gyration in the Θ state. Values of α are reported in the preceding paper.[5] Equation 8 is easy to use. Compared to eq 5, we have only to replace $\bar{u}$ by $\alpha^2\bar{u}$.

However, it would be more appropriate to use a somewhat more realistic distribution than eq 2. Such a distribution was previously proposed by McIntyre,[10] which was reduced from Monte Carlo calculations, but the details are not yet available.

Now, we are able to compare the experimental results with those predicted by the heterogeneous comb model. Values of the inverse of the particle scattering factor $P(q)_z$, computed from eq 6, are plotted versus q^2 together with experimental values, shown by squares, in Figure 1, parts a–c. Best-fit values of n_b are collected in Table II.

We find that with regard to LDPE 1 and LDPE 3 values of n_b agree very well with those presented in ref 5, determined there with respect to the g ratio. In contradiction, the best-fit value of n_b for Lupolen ($n_b > 100$) is about a factor of 10 larger than one estimated by the g ratio. This discrepancy is too high to be sure that Lupolen possesses a structure like a comb. However, the comb model, used here, is relatively simple. To prove this, we need a more realistic model, which will be presented in the next section.

Combs: Monodisperse with Respect to Molar Mass and Polydisperse with Respect to the Length of a Branch

In the preceding section, we have considered comb molecules, where each branch possesses an equal number of segments. Now, we explore comb molecules, which are both monodisperse with regard to the degree of polymerization and monodisperse with regard to the number of total branching points per molecule, but we suppose the number of segments per branch to be an arbitrary distribution. In addition, we keep up the irregular placement of the branches along the backbone.

As a starting point, we utilize the model sketched in Figure 2. The comb molecule contains f branches, divided into groups of f_μ branches, each with n_μ segments, randomly attached to the backbone of N_0 segments. It holds that

$$N = N_0 + \sum_{\mu=1}^{m} f_\mu n_\mu \qquad f = \sum_{\mu=1}^{m} f_\mu$$

N and f are the total number of segments or the total number of branching points per molecule, respectively. m denotes the number of different branch types, which are distinguished by their length.

It is convenient to number chain segments on the backbone serially from 1 to N_0 and in each branch from 1 to n_μ beginning at the junction. The spacing of the branches is specified by the f segments $i_{\mu l}$, where $i_{\mu l}$ denotes the 1st branching point of the backbone that serves as a point of attachment for a branch containing n_μ segments.

Thus we obtain three classes of segment pairs: (a) both segments of the pair j and k on the backbone

$$x_{jk} = |j-k|;\ 1 \le j \le N_0;\ 1 \le k \le N_0$$

(b) one segment on the backbone and one on branch μ_l

$$x_{jk} = |j - j_{\mu_l}| + k;\ 1 \le j \le N_0;\ 1 \le k \le n_l$$

(c) segments j and k on branches μ_l and ν_p confining the case $\mu_l = \nu_p$

$$x_{jk} = |j_{\mu_l} - j_{\nu_p}| + j + k;\ 1 \le j \le n_l;\ 1 \le k \le n_p$$

Here, x_{jk} denotes the number of segments along the chain separating segment j from segment k. In order to obtain an explicit expression for $P(q)$, we make use of eq 3, where

$$N^2 P(\Theta) = \sum_{j}^{N}\sum_{k}^{N} \exp(-t x_{jk}) \qquad t = b^2q^2/6$$

The double summation must be carried out over all combinations of segment pairs, stated above; with $j \neq k$. It follows that

$$N^2P(\Theta) = \left[\begin{array}{ll} \displaystyle\sum_{j}^{N_0}\sum_{k}^{N_0} \exp(-t|j-k|) & \text{(S1)} \\ + 2\displaystyle\sum_{l}^{m}\sum_{\mu_l}^{f_l}\sum_{j}^{N_0}\sum_{k}^{n_l} \exp[-t(|j-j_{\mu_l}|+k)] & \text{(S2)} \\ + \displaystyle\sum_{p}^{m}\sum_{l}^{m}\sum_{\nu_p}^{f_p}\sum_{\mu_l}^{f_l}\sum_{k}^{n_p}\sum_{j}^{n_l} \exp[-t(|j_{\mu_l}-j_{\nu_p}|+j+k)] & \text{(S3)} \end{array}\right] \tag{9}$$

N_0 and N take on values much larger than 1; t takes on a value much smaller than 1. Obviously, the first sum,

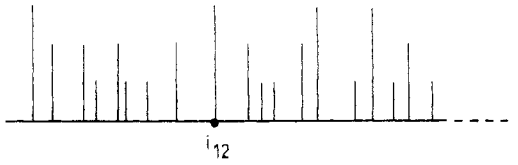

Figure 2. Schematic diagram of a comb molecule constructed from a backbone chain of N_0 chain segments of f branches, where the branches contain different number of segments n.

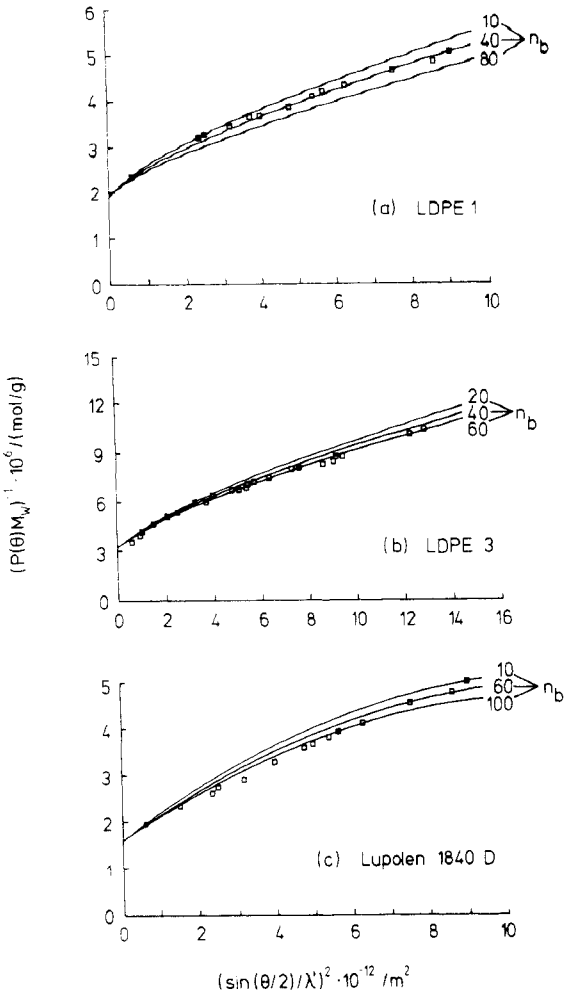

Figure 3. Particle scattering factors calculated by the modified comb model: (a) LDPE 1, (b) LDPE 3, and (c) Lupolen 1840 D.

S1, can be replaced by a double integral. Performing this integration we get

$$S1 = 2\int_0^{N_0}\int_0^{j}\exp(-t(j-k))\,dk\,dj$$

$$S1 = \frac{2}{t^2}(tN_0 + \exp(-tN_0) - 1) = \Psi$$

where Ψ is the well-known Debye function for a linear macromolecule with N_0 segments. The second sum, S2, can be transformed into a 3-fold sum, since $\sum_k^{n_l}\exp(-t(|j - j_{\mu l}| + k))$ is simply a geometric series.

$$S2 = 2\sum_l^m\sum_{\mu_l}^{f_l}\sum_j^{N_0}\exp[-t(|j-j_{\mu_l}|+1)]\left(\frac{\exp(-tn_l)-1}{\exp(-t)-1}\right)$$

The branches are placed at random along the backbone. $j_{\mu l}$ takes on all values between 1 and N_0; thus it is realistic to assume that there is effectively a continuous distribution of $j_{\mu l}$, characterized by the probability f_l/N_0, that any particular segment of the backbone bears a branch. Then in analogy to S1 it follows that

$$S2 = 2\Psi\exp(-t)\sum_l^m\frac{f_l}{N_0}\left(\frac{\exp(-tn_l)-1}{\exp(-t)-1}\right)$$

Assuming stochastical independence for the building of branches at segments on the backbone, the third sum, S3, can be transformed by similar arguments, as stated above, into a double sum. We obtain

$$S3 = \left[2\sum_l^m\sum_p^m\sum_{\nu_p}^{f_p}\sum_{\mu_l}^{f_l}\exp[-(t|j_{\mu_l}-j_{\nu_p}|+2)]\times\left(\frac{\exp(-tn_l)-1}{\exp(-t)-1}\right)\left(\frac{\exp(-tn_p)-1}{\exp(-t)-1}\right)\right]$$

$$S3 = 2\Psi\exp(-2t)\sum_l^m\sum_p^m\frac{f_l f_p}{N_0N_0}\left(\frac{\exp(-tn_l)-1}{\exp(-t)-1}\right)\times\left(\frac{\exp(-tn_p)-1}{\exp(-t)-1}\right)$$

Combining these results with eq 9, we get

$$N^2P(\Theta) = \left[\frac{2}{t^2}(N_0t + \exp(-tN_0) - 1)\times\left[1 + 2\exp(-t)\sum_l^m\frac{f}{N_0}\left(\frac{\exp(-tn_l)-1}{\exp(-t)-1}\right) + \exp(-2t)\sum_l^m\sum_p^m\frac{f_l f_p}{N_0N_0}\left(\frac{\exp(-tn_l)-1}{\exp(-t)-1}\right)\left(\frac{\exp(-tn_p)-1}{\exp(-t)-1}\right)\right]\right] \quad (10)$$

In order to prove eq 10, we let q decrease to zero. If there is no mistake $N^2P(q)$ must be convergence to N^2. In fact, this is the case. It therefore holds that

$$N_0^2\left[1 + 2\sum_l^m\frac{f_l n_l}{N_0} + \sum_p^m\sum_l^m\frac{f_l f_p}{N_0N_0}n_l n_p\right] = N_0^2 + 2N_0\sum_l^m f_l n_l + \sum_p^m\sum_l^m f_l f_p n_l n_p = [N_0 + \sum_l^m n_l f_l]^2 = N^2$$

At the other extreme, when $f = 0$, eq 10 reduces to the Debye function. So, two necessary conditions concerning the applicability of eq 10 are fulfilled. In spite of this, we are able to compare the experimental results for $P(q)_z$ with those computed by eq 10. Then by taking into account the effect of polydispersity and the effect of excluded volume as described above, we get the curves given in Figure 3, parts a–c.

The experimental $P(q)_z^{-1}$ data for LDPE 1 or LDPE 3 are seen to be in good agreement with the theoretical prediction. Best-fit values of n_b, listed in Table II, agree quite well with those estimated by the g ratio. Thus, it seems likely that LDPE 1 and LDPE 3 possess a molecular structure similar to a comb. However, the data of $P(q)_z^{-1}$ and n_b are affected by an error of 1 and 10%. Consequently, it is not possible to decide whether the first or the second comb model describes the experimental data best. Similar results are also obtained when dealing with other kinds of comb structures. This illustrates the limits of utility and meaning which can be attributed to particle scattering factors.

At first sight, the spectrum of Lupolen 1840 D also shows quite good agreement between theory and experiment. However, the best-fit value of n_b is on the order of magnitude of 60 in contrast to the magnitude of 9 derived from the g ratio. Thus, we believe Lupolen pos-

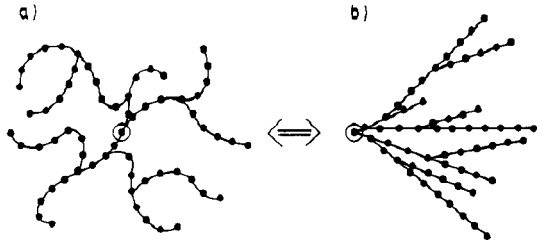

Figure 4. (a) Projection of a coiled polymer tree of the kind A_2–B_x and (b) the topological equivalent tree diagram.

Scheme I

Monomer of the kind A_2–B_x

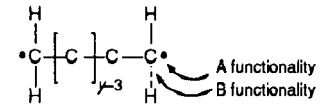

(1) Chain lengthening

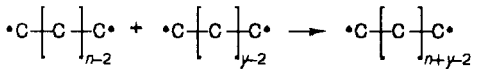

(2) Branching

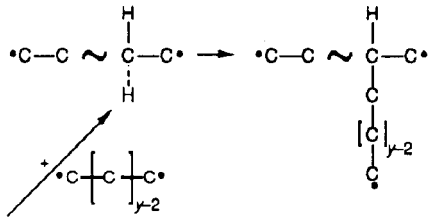

sesses a different kind of branched structure to LDPE 1 or LDPE 3. Structures like stars or rings are unlikely in regard to the mechanism of polymerization of LDPE's. A probable structure according to the preceding paper[5] is that of a polymer tree. A special model, the A_2–B_x polymer tree, will be presented in the next section.

Random Branched Trees of the Kind A_2–B_x

The low-density polyethylene, used here, was obtained by free-radical polymerization. In order to develop a model for this process, we consider a linear chain containing y carbon atoms as a monomer, which possesses at both ends one free electron. An electron may be understood as functionality A and a C–H group as functionality B.

Obviously, we get a monomer of the kind A_2–B_x, where x denotes the number of C–H groups per monomer, which are able to react with an A functionality. Because of steric reasons the value of x is in general smaller than $2y$. The possible reactions during the free-radical polymerization are shown in Scheme I. The extent of branching depends on the conditions of the reaction, e.g. temperature and pressure. At one extreme there will be no reaction of the C–H groups at all, and the effective functionality of the monomer is two. Here, we have no branching, and the resulting macromolecule is a linear one. At the other extreme, the C–H groups react extensively with free electrons. In this case, the branching frequency increases in the course of reaction, and we get a branched structure similar to that sketched in Figure 4.

The probability that a certain functionality A of a polymer tree reacts with a functionality A of a free monomer is concerned with energetic reasons with respect to the small length of the monomer (ethylene; $y = 2$), which is much larger than the probability that functionality A of a tree reacts with functionality B of a monomer. Thus, we have to take into account the reaction A → A, represented by the link probability α, whereas we can neglect the reaction A → B.

Table III

functionality A or B of a tree	reacts	with functionality A or B of a free monomer	with the link probability α, 0, or β
A		A	α
A		B	0
B		A	β
B		B	0

A polymer tree possesses much more functionalities of the kind B than of the kind A. Thus, it is more likely that a free monomer meets a B rather than an A functionality of a tree. A random meeting of two B functionalities does not give a link. Thus, we have only to account for the reaction B → A, which may be represented by the link probability β. The possibilities of reaction and the assigned link probabilities are summarized in Table III.

In order to provide a relationship between the link probabilities and the particle scattering factor $P(q)_z$, we make use of the cascade theory, developed by Good and Gordon.[11] Thereby for simplicity we assume that averaging all subchains of a polymer tree follows Gaussian statistics. It follows that

$$P_w P(q)_z = 1 + (\langle \vec{N}(1) \rangle [(\vec{1} - \mathbf{P}\phi)^{-1}]\vec{1}) \qquad (11)$$

where $\mathbf{P}$ is the transition probability matrix. The matrix $\mathbf{P}\phi$ is of the same form as $\mathbf{P}$ but now the transition probabilities have to be multiplied by factors $\phi_{ij} = \exp(-b_{ij}^2 q^2/6)$, where b_{ij} is the effective bond length between functionality i and j (i, j = A, B). Here b_{ij} is a constant. $\langle \vec{N}(1) \rangle$ denotes a vector, which contains the population number of the root linked segments in the first generation of a polymer tree. P_w denotes the weight-average degree of polymerization.

In order to construct $\langle \vec{N}(1) \rangle$ and P we make use of probability-generating functions.[12] First, we consider functionality A. The distribution of reactants is very simple because there is only one probability (functionality A has bound another monomer) and a probability $1 - \alpha$ (no monomer is bound). The definition of a generating function requires that the probability for no event has to be multiplied by $S_A^0 = 1$, and the probability for one event by $S_A^1 = S_A$; hence, the probability-generating function for functionality A is given by

$$F_A(\vec{S}) = 1 - \alpha + \alpha S_A$$

In an analogous manner we get the probability-generating function for the functional group B. It holds that

$$F_B(\vec{S}) = 1 - \beta + \beta S_A$$

The monomer segment chosen as root bears two functional groups of the kind A and x functional groups of the kind B. Thus, the distribution of offspring is 2-fold with respect to the x-fold convolution of the functional group probability. It follows that

$$F_0(\vec{S}) = ((1 - \alpha) + \alpha S_A)^2 (1 - \beta + \beta S_A)^x$$

where $F_0(\vec{S})$ is the generating function of the polymer root.

A monomer in the first generation of a polymer tree, or in any higher generation, has only one functionality of the kind A but x functionalities of the kind B available for further reactions. In addition, the transition prob-

ability $w_{A\to B}$ is equal to zero. Thus we can write

$$F_{1A}(\vec{S}) = ((1-\alpha) + \alpha\vec{S}_A)\,(1-\beta+\beta\vec{S}_A)^x = F_{nA}$$

$$F_{1B}(\vec{S}) = 1 = F_{nB},\ \mathrm{d}a\ w_{A\to B} = 0$$

where $F_{1A}(\vec{S})$ and $F_{1B}(\vec{S})$ are the generating functions with respect to the first generation. Now, it is simple to calculate the expression for $\langle\vec{N}(1)\rangle$, $\mathbf{P}$, and $(1-\mathbf{P}\phi)^{-1}$, which are listed below.

$$\langle N(\vec{1})\rangle = \left(\frac{\partial F_0}{\partial s_A}(\vec{1}) \quad \frac{\partial F_0}{\partial s_B}(\vec{1})\right) = (2\alpha + x\beta \quad 0)$$

$$\mathbf{P} = \begin{pmatrix} \frac{\partial F_{1A}}{\partial s_A}(\vec{1}) & \frac{\partial F_{1A}}{\partial s_B}(\vec{1}) \\ \frac{\partial F_{1B}}{\partial s_A}(\vec{1}) & \frac{\partial F_{1B}}{\partial s_B}(\vec{1}) \end{pmatrix} = \begin{pmatrix} \alpha + x\beta & 0 \\ 0 & 0 \end{pmatrix}$$

$$(1-\mathbf{P}\phi)^{-1} = \frac{1}{1-(\alpha+x\beta)\phi}\begin{pmatrix} 1 & 0 \\ 0 & 1-(\alpha+x\beta)\phi \end{pmatrix}$$

Introducing these expressions into eq 11, we get the final result.

$$P_w P(q)_z = (1+\alpha\phi)/(1-(\alpha+x\beta)\phi) \qquad (12)$$

Further it follows that

$$P_w = \lim_{q\to 0} P_w P(q)_z = (1+\alpha)/(1-(\alpha+x\beta)) \qquad (13)$$

$$\langle S^2\rangle_z = -3\mathrm{d}P(q)_z/\mathrm{d}q^2 = b^2 P_w(2\alpha+x\beta)/(2\,(1+\alpha)^2) \qquad (14)$$

In order to compare the results, predicted by eq 12, with those of the experiment, the values of the link probabilities α and β must be known. We get them by solving eq 13 and 14 with respect to P_w and $\langle S^2\rangle_z$. Values of P_w and $\langle S^2\rangle_z$ are reported in ref 5. Figure 5, parts a–c, show the pertaining plots. For comparison, the particle scattering factor of a heterogeneous comb is also pictured.

The most striking feature concerning polymer trees of the kind A_2–B_x is the strong upward curvature of $P(q)_z^{-1}$, in divergence to the experimental data. With regard to LDPE 1 and LDPE 3 this can be interpreted as justification for the comb hypothesis. However, we could expect a better agreement between theory and experiment for Lupolen 1840 D. The standard deviation of $P(q)_z^{-1}$ is just as large as those estimated for the comb models. Despite this, it is possible to get a quite good fit for the spectrum of Lupolen. We have only to superimpose the $P(q)_z^{-1}$ function representing a heterogeneous comb with those representing a polymer tree of the kind A_2–B_x, each weighted by the factor 0.5. Figure 6 shows this fit. Consequently, Lupolen possesses a branched structure, which seems in some details to be a comb and in some others to be a tree.

Finally, we have to prove whether our results are consistent with those presented in the preceding paper.[5] There we have stated that two dissolved Lupolen molecules, if they meet together, can interpenetrate each other somewhat less than two LDPE 1 or LDPE 3 molecules can. The next section, dealing with the segment-density function, will examine this statement.

Correlation Functions

The concept of correlation functions was introduced by Debye and Bueche[13] in order to describe inhomogeneities in solid material. In dilute solutions, observed here, the motion of molecules can be assumed to be completely independent from each other, and under these circumstances the correlation function $\gamma(r)4\pi r^2\,\mathrm{d}r$ is the probability of finding another segment of the same molecule in the spheric shell of r and $r+\mathrm{d}r$, if the reference segment is at position $r=0$. Outside the molecule domain $\gamma(r)$ is equal to zero. Often, $\gamma(r)$ is called the segment-density distribution, which states that molecules of equal size but of different molecular structure must be associ-

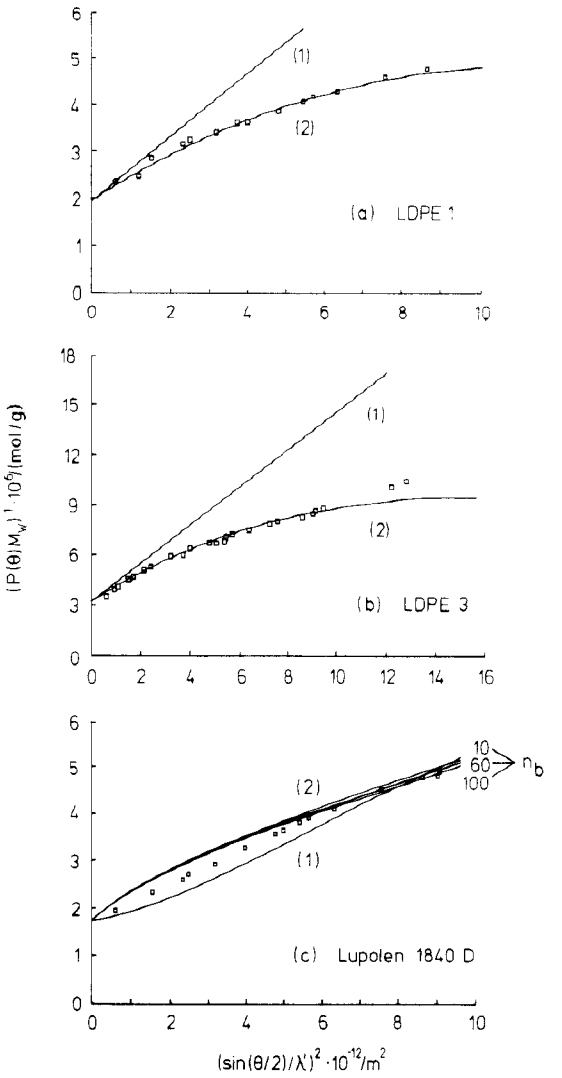

Figure 5. Particle scattering factors calculated by the A_2–B_x tree model: (a) LDPE 1, (b) LDPE 3, and (c) Lupolen 1840 D, (1) polymer tree and (2) heterogeneous comb.

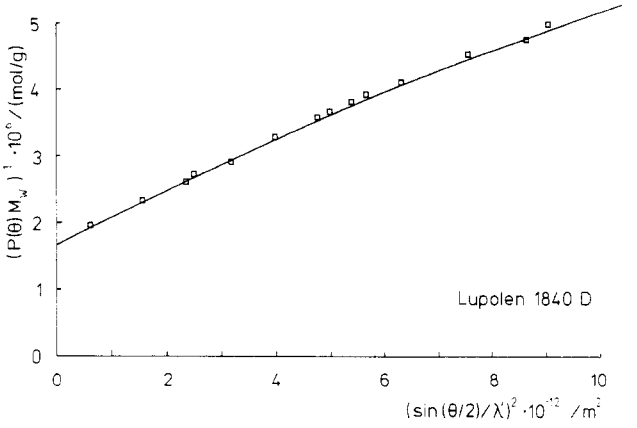

Figure 6. Lupolen 1840 D: particle scattering factor attained by superimposement of $P(q)$ factors describing a heterogeneous comb and a A_2–B_x tree.

ated with different segment-density distributions. $\gamma(r)$ can be calculated by application of the Fourier theorem to the particle scattering factor. It holds that

$$(2\pi)^3 r\gamma(r) = \int_0^\infty P(q)_z \sin(qr)\, dq \qquad (15)$$

Expressions for $P(q)_z$, which yield an excellent fit with regard to the LDPE's, studied here, are listed below.

sample	best-fit expression for $P(q)_z$
Lupolen 1840 D	$P(q)_z = 1 - {}^1/_3\langle S^2\rangle_z q^2$
LDPE 1; LDPE 3	$P(q)_z = (1 + Aq^2)^{-0.5}$

$\langle S^2\rangle_z$ is the mean-square radius of gyration. A denotes a parameter, which is equal to ${}^2/_3\langle S^2\rangle_z$. Curves of $P(q)_z$ are pictured in Figure 7, parts a–c.

Equation 15 for Lupolen 1840 D gives

$$\gamma(r) = ({}^3/_2)\pi^{-5/2}(r\langle S^2\rangle_z)^{-1/2} \exp(-(3/\langle S^2\rangle_z)^{0.5} r)$$

With regard to LDPE 1 and LDPE 3 we find that

$$\gamma(r) = ({}^3/_4)\pi^{-7/2}(r\langle S^2\rangle_z)^{-1/2} K_1(r/(({}^2/_3)\langle S^2\rangle_z)^{0.5})$$

where $K_1(r)$ is MacDonald's function of the first kind. Values of $K_1(r)$ are tabulated in the literature.[14]

Plots of $4\pi r^2\gamma(r)$ versus r are shown in Figure 8. In general, it is not simple to interpret the curvature of a correlation function. Fluctuating between different molecules will be correlated and will give rise to interparticle scattering. Therefore, the apparent mean-square radius of gyration due to eq 15 will be larger than that of the isolated molecule. For instance, aggregates will behave like branched molecules, and $\langle S^2\rangle_z$ will be that of the aggregate.

Here, it can be seen that the correlation function of Lupolen 1840 D is much more broader than one of LDPE 1 or LDPE 3. A possible conclusion may be stated as follows.

Previously, we showed that (1) LDPE 1 and LDPE 3 possess a molecular structure, which can be described quite well as being comblike, and (2) that the molecular structure of Lupolen 1840 D lies somewhere between a comb and one of a tree. Figure 9, parts a and b, illustrates this idea.

Now, taking these sketches as a base, we may draw imaginary circles at distances of dr around the centers of mass. This yields circle shells, each occupied with a definite number of segments. Then, we plot the number of segments per shell against the radius of the pertaining circle. The result presents to a first approximation the segment-density function $\gamma(r)r^2$ dr. Doing so, we come to the result that the segment-density function of Figure 9b (Lupolen 1840 D) is broader than those of Figure 9a (LDPE 1 or LDPE 3), a result which is consistent with the experiment.

Finally, we can inspect the problem of interpretation. According to Figure 9, the segment density in a unit volume is larger for Lupolen than for LDPE 1 or LDPE 3. Thus, two Lupolen molecules will hinder each other more, if they try to interpenetrate, than two LDPE 1 or LDPE 3 molecules will. Consequently, the degree of interpenetration is higher for LDPE 1 or LDPE 3 than for Lupolen 1840 D, which is consistent with the statement of the preceding paper.

Conclusions

(1) In the paper presented here, particle scattering factors, based on models for different branched molecular structures, were calculated and compared with experimental results, derived for some low-density polyethylenes. Values of $P(q)_z$, computed with respect to both of

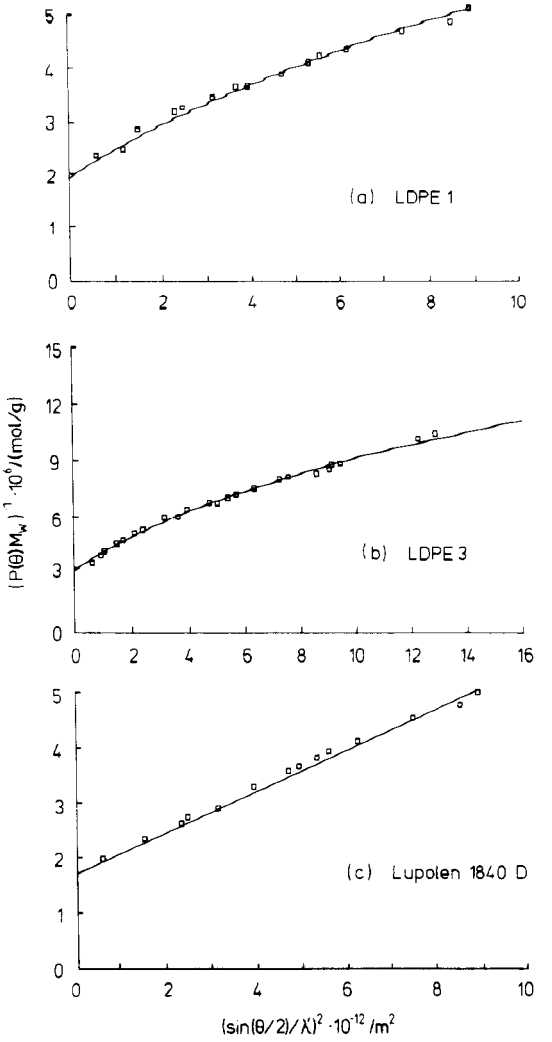

Figure 7. Particle scattering factors calculated by correlation functions: (a) LDPE 1, (b) LDPE 3, and (c) Lupolen 1840 D.

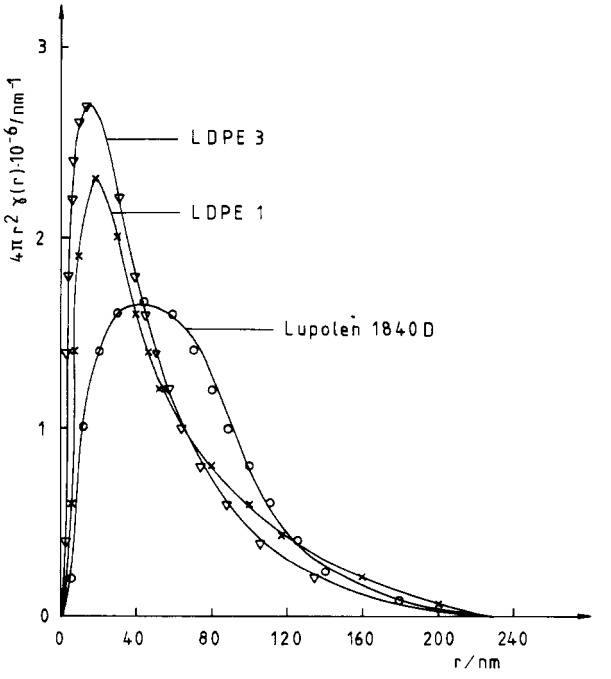

Figure 8. Correlation functions.

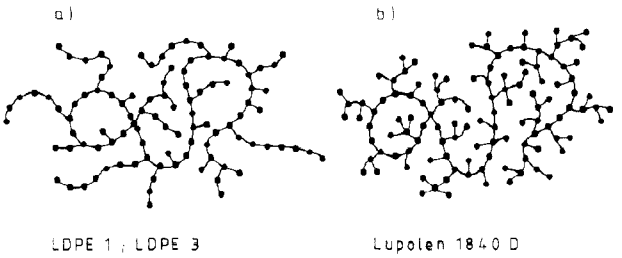

Figure 9. Proposed molecular structures: (a) LDPE 1 or LDPE 3 and (b) Lupolen 1840 D.

the comb models, agree well with the experimental data with regard to LDPE 1 and LDPE 3. However, the accuracy of the experimental data is not of a high enough order to decide which of the comb models describes the spectra best. The theoretical predictions concerning Lupolen 1840 D are in somewhat poorer agreement with experiment. A quite good fit of $P(q)_z^{-1}$ is obtained by a superimposement of the particle scattering factor, describing a comb molecule with one describing a polymer tree of the kind A_2–B_x. Confirmation according to this supposition will be attained from an analysis of the correlation function, which states that the segment density of a Lupolen molecule is larger than that of a LDPE 1 or LDPE 3 molecule. This is consistent to the finding that two LDPE 1 or LDPE 3 molecules are less hindered than two Lupolen molecules, if they try to interpenetrate each other.

(2) The models, presented here, incorporate the effect of excluded volume in a somewhat simple manner. We have used the relationship $\langle r_{ij}^2 \rangle = \alpha^2|i - j|b^2$. On the other hand, we get by this procedure values for n_b, concerning the number of segments per long branch, which are in good agreement with those derived in the previous paper.[5] However, further calculations are planned to prove this statement.

(3) As has been shown in preceding sections of this paper, the particle scattering factor $P(q)_z$ or its reciprocal $P(q)_z^{-1}$ can, in principle, yield important information on the size, shape, and polydispersity of scattering particles. The theory of evaluating $P(q)$ factors has been developed to a rather high degree of perfection. The limiting factor in applying the achievements of the theory is its failure to analyze successfully the scattering behavior of systems in which the influence of more than one effect is operative and unknown simultaneously. For instance, conclusions concerning the shape of dissolved macromolecules can be drawn only with systems consisting solely of particles of the same shape and exactly known polydispersity of molecular mass. Otherwise the individual effects superimpose on each other, and there is hardly any way to discriminate their contributions. It is rather deplorable, but certainly the case, that care in interpreting the $P(q)_z^{-1}$ functions in terms of particle shape and polydispersity cannot be overemphasized. Therefore, all interpretations concerning particle shape should be proved by other physical methods. We, for instance, plan to perform neutron, synchrotron, and dynamic light scattering measurements in order to confirm our results.

(4) Finally, a few comments have to be made about the calculation techniques used here. The stochastical theory of cascade processes presents a relatively comfortable technique in computing particle scattering factors. Much more complicated models can be treated from the conditions of a chemical preparation than by use of Debye's technique. Nevertheless, some doubt may be allowed, whether this theory takes correctly into account the effect of polydispersity, namely, the true form of the molar mass distribution. In order be certain and avoid this difficulty, it may be better to use Debye's technique. The best agreement between experiment and theory will be obtained by working with correlation functions, which often allows an immediate qualitative interpretation of scattering curves without time-consuming model calculations. However, correlation functions comprise the effects of intra- and interparticle scattering, which limits its application.

Summarizing these considerations we conclude that each technique reported here has both its advantages as well as its disadvantages, which emphasizes that in practice one cannot ignore neither the one nor the other concept.

References and Notes

(1) Debye, P. *J. Phys. Colloid Chem.* **1947**, *51*, 18.
(2) Gordon, M. *Proc. R. Soc. London, A* **1962**, *268*, 240.
(3) Stauffer, D. *Phys. Rep.* **1979**, *54*, 1.
(4) Stauffer, D.; Coniglio, A.; Adam, M. *Adv. Polym. Sci.* **1982**, *44*, 103.
(5) Nordmeier, E.; Lanver, U.; Lechner, M. D. *Macromolecules*, preceding paper in this issue.
(6) Casassa, E. F.; Berry, G. C. *J. Polym. Sci., Polym. Phys. Ed.* **1966**, *4*, 881.
(7) Brandrup, J.; Immergut, E. H. *Polymer Handbook*; Wiley: New York, 1975.
(8) Ptitsyn, O. B.; Benoit, H. *Zh. Fiz. Khim.* **1957**, *31*, 1091.
(9) Smith, T. E.; Carpenter, K. *Macromolecules* **1968**, *3*, 204.
(10) McIntyre, D.; Mazur, J.; Wims, A. M. *J. Chem. Phys.* **1968**, *49*, 2887.
(11) Burchard, W.; Patterson, G. D. *Advances in Polymer Science 48*; Springer: New York, 1983.
(12) Feller, W. *An Introduction to Probability Theory and its Applications*; Wiley: New York, 1968.
(13) Debye, P.; Buecke, A. M. *J. Appl. Phys.* **1949**, *20*, 518.
(14) Bronstein, I. N.; Semendjajew, K. A. *Taschenbuch der Mathematik*; Harri Deutsch: Frankfurt/Main, 1981.

Registry No. Lupolen 1840D, 9002-88-4.